Mapping the Spatiotemporal Diversity of Precipitation in Iran

Zahra Jamshidi
Shiraz University
Nozar Samani (samanin@shirazu.ac.ir)
Shiraz University https://orcid.org/0000-0003-3959-8612

Research Article

Keywords: Precipitation, Iran, Climatological zone, Principal component analysis, Hierarchical clustering, K-Means clustering

Posted Date: November 3rd, 2021

DOI: https://doi.org/10.21203/rs.3.rs-1036520/v1

Abstract

Despite located in a semi-arid and arid part of the world, Iran enjoys a very diverse climate. As a result, water availability in different regions of the country is in a veil of ambiguity. To have a better insight, we investigate the spatiotemporal diversity of precipitation over the country by analyzing the 33-years long monthly precipitation time series (1983-2016) at 461 measuring rain-gauge stations. Cluster Analysis (CA) both hierarchical and non-hierarchical clustering approaches and Principal Component Analysis (PCA) was used to determine the homogeneous precipitation zones at three macro, meso, and micro-scales. First, the country is divided into six precipitation macro-regions using CA. Each region shows a unique mean annual hyetograph and is influenced by a particular air moisture mass entering the country. Then, the six regions were divided into 10 regions of meso-resolution through Hierarchical clustering (HC) and K-Means Clustering. Finally, an optimal number of 24 micro-zones is established that reflect a comprehensive precipitation map over the country, employing PCA, Hierarchical clustering, and K-Means Clustering. The annual hyetograph of each zone showed a unique pattern and distribution with a varying magnitude of monthly precipitation compared to others. The long-term (i.e., 33-years) mean annual rainfall in each region and zone is calculated, and the monthly and annual-precipitation water availability in the country is estimated. The result gives an accurate insight into the amount of precipitation that is expected to fall in each zone during each month of the year, that may be used as the reference for the prediction of the dry and wet seasons and years and also for the allocation of the harvested precipitation water to different consumptive sectors. The result shows that the Hierarchical clustering and PCA have significant classification performance in meso and micro- climatological zoning. Also, it was observed that there are significant similarities between the PCA and Hierarchical clustering (Ward's method-Pearson correlation) results in micro-climatological zoning.

1. Introduction

Precipitation is the main component of the water cycle and the sole source of fresh water on the Earth, ignoring the polar ice. Spatiotemporal diversity of precipitation in terms of duration and intensity creates many challenges in the world (Hong et al. 2007; Kidd and Huffman 2011). Latitude, longitude, topography, and location of the land relative to large water bodies (i.e., seas and oceans) are the main factors affecting the intensity, duration, and variation of precipitation. Determining the homogeneous precipitation zones at different scales is essential for water resources management. Precipitation and climatological zoning have long been of interest to researchers around the world. Köppen was the first researcher who classified the world climate in 1900 based on vegetation, temperature, and humidity (Kottek et al. 2006). Many regional investigations have been performed on climatological zoning in the world (Mills, 1995; Baeriswyl and Rebetez, 1997; Gocic and Trajkovic, 2014; Uddin et al. 2019; Srivastava et al. 2019; Knerr et al. 2020; Ribes et al. 2020; Dinpashoh et al. 2004; Modarres and Sarhadi, 2011; Raziei, 2018; Alizadeh et al. 2019). In Iran, Domroes et al. (1998) prepared 31-year monthly rainfall records (1957-1987) at 71 rainfall stations and identified five precipitation zones using two methods of principal component analysis (PCA) and cluster analysis (CA). Modarres (2006) used the Hierarchical cluster analysis of annual and monthly precipitation of 28 main towns of Iran and recognized eight homogeneous precipitation regions. Soltani et al. (2007) fitted the monthly precipitation time series of 28 cities into ARIMA (Auto-Regressive Integrated Moving Average) models and by PCA and CA determined three simple, moderate, and complex climate regions in Iran. Sarmadi and Shokoohi (2015) obtained eight precipitation regions over Iran based on the standardized precipitation data from 1951 to 2007, using two multivariate methods of factor analysis (FA), and CA. Samani and Karimi (2009) applied PCA on the 29 years monthly rainfall from 44 synoptic stations in Iran and showed that the first ten components forming about 63 % of the total variance of the rainfall data and classified Iran into nine climatological zones. Darand and Daneshvar (2014) applied PCA and CA on eight seasonal rainfall–based variables (1951 to 2007) and identified ten rainfall regimes in Iran and reporting the winter season as the main rainfall period.

The climatological zoning will be different and depends on the number of stations, the period of precipitation data, and the procedure of analysis. Air masses entering the country, varied topography, extensive area of the county, and extensive nearby water bodies create a very diverse climate in Iran. In this paper, we attempt to homogenize the spatiotemporal diversity of precipitation over Iran in three macro, meso, and micro scales, using PCA, hierarchical and non-hierarchical clustering. The homogenized precipitation zones provide useful information on the water availability in each zone for water resources management in the country. In addition, the relative potential of statistical approaches in differentiating the precipitation zones is highlighted. The paper is organized as follows: Section 2 described the study area and data used. The methodology is explained in section 3. In section 4, we introduced the results and discussion. Section 5 presents the conclusion.

2. Materials

2.1 Study area

Iran is a country located in West Asia with an approximate area of 1648195 km^2 within the latitude of 25°–40° N and longitude of 44°–64° E, bordered by the Caspian Sea to the north and the Persian Gulf and the Oman Sea to the south. Iran's neighbors are Afghanistan and Pakistan in the east; Turkmenistan, Azerbaijan, and Armenia in the north; Turkey and Iraq in the west; and the Arab States of the Persian Gulf in the south (Fig. 1). Iran has a varied topography. Mount Damavand (5,671 m above the m.s.l.) and the southern coast of the Caspian Sea (28 m below the m.s.l.) is the highest and lowest point in the country, respectively (Madani, 2014). Dasht-e-Lut and Dasht-e-Kavir are two major deserts that cover the central part of the country. Two high mountain ranges of Iran are Alborz and Zagros in north and west, respectively, which cause the low rainfall in the interior of the country (Alijani et al., 2008; Balling et al., 2016; Vaghefi et al., 2019). Iran has a varied climate, often arid or semi-arid, characterized by high evapotranspiration potential and low rainfall. Annual precipitation is lower in the eastern half of Iran in comparison with the western half (Nazemosadat et al., 2006). Annual precipitation varies from over 1000 mm on the west coast of the Caspian Sea and the western highlands to less than 50 mm in uninhabitable eastern

deserts. The average annual rainfall across the country is estimated equal to 250 mm, which is less than a third of the global average annual rainfall. Winter is the season with the heaviest rainfall, and only a few regions of the country (Caspian Sea coast, northwest, and southeast) receive rain in summer. The temperature varies from -20 to +50°C throughout the country. The hottest and coldest months of the year are July and January with average temperatures of 19 to 39°C and 6 to 21°C in most parts of the country, respectively. Significant spatial and temporal variability of rainfall in Iran has been the motivation for the construction of large dams and reservoirs to regulate water flow (Madani, 2014).

2.2 Data

The daily precipitation records of 404 rain gauges and 57 synoptic stations were collected from the archive of the Regional Water organization and Meteorological Organization of Iran (461 stations in total) for 1983 through 2016. The daily data in each month of the year were aggregated to form the monthly precipitation time series. The location of these stations is shown in Fig. 1. It should be noted that there are over 1450 rain gauges in Iran. However, we selected the 461 stations with the longest (i.e., 33 years) of continuous records.

3. Methodology

We employed CA and PCA to classify the spatiotemporal regimes of precipitation in Iran. CA is a statistical method for classifying sample data into clusters such that each cluster is of high similarity and a sharp and distinct difference between clusters exists. CA includes hierarchical and non-hierarchical clustering approaches (Fovell and Fovell, 1993). Hierarchical Clustering Analysis (HCA) constructs a hierarchy of clusters, a cluster tree or dendrogram starting with each point (record) as a single cluster, and then repeatedly merging the most similar pair of clusters until reaching a single all-encompassing cluster (Everitt et al. 2001; Rencher 2002). HCA was applied, using Euclidean distance and Pearson correlation as similarity measures and Ward's method as the linkage rule to classify the precipitation data. K-Means Clustering (MacQueen, 1967) is one of the non-hierarchical clustering (partitioning clustering) procedures and the most often uses an unsupervised machine learning algorithm for dividing a data set into a set of K clusters (Kassambara, 2017). CA is performed on the data using IBM SPSS Statistics and R software.

PCA is one of the simplest and the best methods of data analysis that is widely used in climatology (Ehrendorfer, 1987; White et al. 1991). PCA reduces a large matrix of data to several main components or principal components (PCs). The first PC explains the main part of the total variance of a data set and the next components explain a smaller portion of the remaining variance successively. PCs are the eigenvectors of a variance-covariance matrix and PCA is the technique that attempts to reveal the underlying latent structure which exists within a series of data set. Only those PCs that have eigenvalues greater than one or explain a specified % of the total variance, usually above 65%, are significant and will be selected for interpretation (Davis 2002; Candeias et al. 2011). PCA was performed on the monthly precipitation data using IBM SPSS Statistics, and the number of components was determined using eigenvalue, % of the total variance, and score plots. Then, the Varimax orthogonal rotation method was used to simplify the interpretation of non-rotating principal components (Richman, 1986; Domroes et al., 1998).

4. Results And Discussion

4.1 Precipitation diversity in macro-scale

The precipitation time series introduced in section 2.2 were subjected to CA, and the results are presented in Fig. 2. Based on Ward's method and Pearson correlation, the precipitation regimes in Iran are spatially classified into six distinct regions, which we call the macro-precipitation regions (MPR) of Iran. The mean annual hyetographs of the six regions illustrated in Fig. 2 show that precipitation in each region has a unique temporal distribution, sharply different from that of the others. The long-term mean annual precipitation depth in the six regions $(\bar{P})$ is plotted in Fig. 3. The MPR1 along the Caspian Sea with a mean annual precipitation of 885 mm and the southeastern desert provinces (MPR6) with 158 mm are the wettest and driest regions, respectively. Considering the moisture air masses entering the country, it seems that the spatial diversity of precipitation is greatly controlled by these air masses. Siberian cold continental air mass (known as (cP) air mass) enters from the north and is blocked by the Alborz Mountain ranges carries moisture from the Caspian Sea provides heavy precipitation in MPR1. The Sudan air mass enters from the south and southwest of the country carrying moisture from the Arabian Sea, the Red Sea, the Persian Gulf, and the Oman Sea (Alijani, 2000; Heydarizad et al. 2018) influences the precipitation regime in MPR2. The Mediterranean air mass affects the precipitation regime in MPR3. North Atlantic and Black Sea cyclones (Sabziparvar et al., 2015) being rich in humidity and entering from the northwest direction provide precipitation in MPR4.

The precipitation regime of MPR6 is controlled by the Maritime Polar air mass (mT) entering the country from the southeast direction (Indian ocean and Oman Sea). While the Mediterranean air moisture influences the precipitation regime of MPR5 but due to the desert nature of this region, the precipitation amount is considerably less than that of MPR3.

Table 1 presents the similarity between our classification and the previous ones. For example, MPR4 corresponds to zone 1, G3, and D of Domroes et al. (1998), Modarres (2006), and Samani and Karimi (2009), respectively.

Table 1
The Similarity between our classification and the previous ones in macro and meso scale.

Scale	This research	Domroes et al. (1998)	Modarres (2006)	Samani and Karimi (2009)
MPR	MPR_1	2 and East part of 1	G_6, G_8	C
	MPR_2	-	G_4, G_7	H, I
	MPR_3	3	G_2, G_5	A
	MPR_4	1	G_3	D
	MPR_5	-	G_1	B, E
	MPR_6	-		F, G
Meso-precipitation zone	A	2	G_8	C
	B	East part of 1	G_6	
	C	-	-	H
	D	3	West part of G_2, G_5	A
	E	-	-	I
	F	West part of 1	G_3	D
	G	-	-	B
	H	-	-	G
	I	-	-	E
	J	-	-	F

4.2 Precipitation diversity in mesoscale

In the previous section, we demonstrated that Iran's precipitation regime is dividable into six regions, mainly as the result of the moist air masses entering the country. However, due to vast area, complex topography, large latitude variations, and extensive nearby water bodies, its variabilities are more complex, so we examined the six regions to see if we can cluster them into more sub-regions. For this, the Hopkins statistic (Lawson and Jurs, 1990) was used. The Hopkins value for the 461 rain gauge stations is determined in the range of 0.65-0.80, indicating that the data are further groupable. The Gap Statistic method was also used to determine the optimal number of clusters for both hierarchical and K-Means Clustering. As presented in Fig. S1 (S stands for Supplementary Materials), the optimum number of groups is 10.

Also, we used the Sdbw index from the NbClust package (Charrad et al., 2012) for determining the optimal number of clusters for hierarchical and K-Means Clustering. All tests demonstrated that the optimal number of groups is ten. Figure S2 depicts the cluster dendrogram of 461 stations. Meso-precipitation zones of Iran based on Ward's method-Euclidean distance and K-Means Clustering are shown in Fig. 4. The ten clusters (A to J) resulted from Ward's method-Pearson correlation mapped on Fig. 5 present Iran's precipitation diversity in a mesoscale. We chose the meso-precipitation zones according to Ward's method-Pearson correlation since it gives the best distinct classification (Fig. 5 compared to Fig. 4). Also, the long-term (1983-2016) mean annual hyetograph in zones A to J are plotted in Fig. 5. The mean annual precipitation in each zone is shown in Fig. 6. Zone A and J have the maximum (1293 mm) and minimum (123 mm) mean annual precipitation, respectively. Comparing Fig. 4 with Fig. 5, it is observed that zone MPR3 (Southwestern region) is divided into zones C and E. It is most probably due to the collision of the Mediterranean and the Sudan air masses. Similarly, MPR6 (Southeastern region) is divided into Zones H and J as the result of the occasional merging of the Sudan air mass with the Maritime air mass entering the country from the southeast direction (Indian ocean and Oman Sea). The similarity between our mesoscale precipitation zoning and the previous ones is tabulated in Table 1.

4.3 Precipitation diversity in Micro-scale

In the next step, we examined the possibility of division of each of the ten mesoscale zones (i.e., A to J) into smaller, rigorous homogeneous sub-zones. For this, several statistical indices from the NbClust package (Charrad et al. 2012) are tested to define the optimum number of sub-zones (micro-zones) in each of the ten mesoscale zones for K-Means Clustering and HCA and the Kaiser-Meyer-Olkin (KMO) criteria and Bartlett's test, the total variance, eigenvalue, and score plot for PCA. Table S1 presents the statistical tests that indicated the same optimal number of micro-zones in each zone. The result of all tests was significant at a p-value= 0.05. As can be observed in the last column of Table S1, except for zone A, zones B, F, H, and J are dividable into two sub-zones, zones C, D, and E to three sub-zones, and zone G to four subzones. In other words, the spatiotemporal regime of Iran's precipitation is classified into 24 micro-zones. Therefore, K-Means Clustering and HCA resulted in the 24 micro-zones that are shown in Figs. 7a, 7b and 7c and their dendrograms are plotted in Fig. S3.

The Kaiser-Meyer-Olkin (KMO) measure of sampling adequacy is a standard test procedure to determine the suitability of using factor analysis (Kaiser, 1970). The KMO measure of sampling adequacy of nine meso-zones (B to J) was found greater than 0.95 (Table S2), above the generally recommended value of 0.60.

Bartlett's test of sphericity (Bartlett, 1950) is applied for testing the null hypothesis that the variables of the correlation matrix are uncorrelated. The results of Bartlett's test of Sphericity for the nine meso-zones (B to J) were found significant ($p<0.0001$), Table S2.

Table S3 reveals the Eigenvalues, % of the variance and cumulative % of different factors in the non-rotational and rotational states. The number of components was extracted from the eigenvalue and the total variance of the components. Only those PCs with an eigenvalue greater than 1.0 that together explain more than 65 % of the total variances of the data was selected. In zones, B, F, H, I, and J the first two PCs together accounted for 65, 73, 78, 80, and 67 percent of the total variance, respectively. In zones, C, D, and E the first three PCs together accounted for 85, 79, and 92 % of the total variance, respectively. In zone G, the first 4 PCs explain 80% of the total variance. Although in zone B and J the total variance is less than 70 %, however, their eigenvalues are greater than 1.0. Therefore, PCA distinguishes 24 precipitation micro-zones the same as K-Means Clustering and HCA.

Score plots of PC1 vs PC2 for zones B to J are presented in Fig. S4, also shows the division of zones B to J into the same number of sub-zones.

The 24 micro-zones are mapped in Fig. 7a, Fig. 7b, Fig. 7c, and Fig. 7d based on K-Means Clustering, HCA (Ward's method-Euclidean Distance), HCA (Ward's method-Pearson correlation), and PCA method, respectively. The results of the four methods are closely similar. However, PCA gives more distinct zoning (Fig. 7d). The formation of 24 micro-zones is due to the vast area, complex topography, large latitude variations of the country, and also extensive nearby water bodies. The mean annual hyetographs of the 24 zones are plotted in Fig. 8 elucidating that while the pattern of the lon-term mean annual hyetograph of micro-zones in each zone (meso-zone) is the same, however, their monthly precipitation magnitude varies. The mean annual precipitation in each micro-zones is shown in Fig. 9. Micro-zone A and J_2 have the maximum (1293 mm) and minimum (99 mm) mean annual precipitation, respectively. To better differentiate the 24 micro-zones visually, and to calculate the precipitation volume, Fig. 7d is plotted on a 0.25°grided map of Iran (Fig. 10). The limiting border of each micro-zone was approximately drawn with the help of the mean annual hyetograph of rainfall stations with a lower number of rainfall records (i.e., less than 33 years) and their similarity with the hyetographs of Fig. 8.

4.4 Annual precipitation volume

The estimated long-term (33 years) mean monthly and annual precipitation in micro-zones is presented in Table 2. Each annual precipitation multiplied by its corresponding area (2rd column of Table 2), and the annual precipitation water volume was calculated as tabulated in the last column of Table 2. The summation of the last column that equals 406 BCM is the precipitation water that Iran receives annually. Note that the area of each micro-zone was calculated from Fig. 10.

Table 2
The mean monthly and annual precipitation and mean annual precipitation water volume in the 24 micro-zones.

Zone	Area (km^2)	Precipitation (mm)												Annual Precipitation (mm)	Annual precipitation water volume (BCM)
		Oct	Nov	Dec	Jan	Feb	Mar	Apr	May	Jun	Jul	Aug	Sep		
A	17342	209.9	187.5	150.4	94.4	101.9	94.7	72.9	59.4	45.3	65.0	54.3	157.3	1293	22.42
B1	15656	91.7	89.6	91.0	61.9	66.2	64.9	50.1	38.2	29.2	39.3	34.8	70.0	727	11.38
B2	23663	38.5	47.4	53.9	42.3	59.1	64.5	60.4	50.4	25.9	24.1	26.8	30.1	523	12.38
C1	34973	5.4	65.9	112.7	101.4	101.3	96.8	87.1	35.0	1.8	0.4	1.0	1.1	610	21.33
C2	52661	3.2	38.5	93.2	95.4	82.1	74.7	68.4	19.4	0.9	0.6	1.1	0.7	478	25.19
C3	71079	2.8	35.6	75.9	71.8	52.4	45.4	38.4	11.8	0.1	0.0	0.4	0.5	335	23.83
D1	22755	12.3	45.8	51.4	36.6	51.7	52.7	59.7	44.2	13.5	10.0	6.9	8.8	394	8.95
D2	91735	8.5	54.1	58.3	45.6	54.5	56.4	60.8	39.6	3.5	0.7	0.6	1.0	384	35.20
D3	55901	11.4	47.6	42.2	31.1	39.0	41.0	54.7	45.7	11.0	4.7	2.6	3.3	334	18.68
E1	47346	1.7	25.1	77.2	90.2	74.3	55.8	49.4	13.7	0.6	0.6	1.4	0.8	391	18.51
E2	45923	0.5	9.7	52.6	61.9	48.7	42.5	31.6	7.7	0.8	0.9	3.8	1.5	262	12.04
E3	25934	1.1	22.2	61.3	68.6	39.0	20.1	16.0	3.8	0.0	0.2	0.6	1.1	234	6.07
F1	74842	14.6	47.9	34.7	28.0	33.7	40.0	51.5	49.2	11.3	4.5	1.9	2.6	320	23.94
F2	62028	16.5	33.5	22.4	16.6	21.6	27.1	39.7	52.3	22.0	11.2	5.6	7.0	275	17.08
G1	30514	9.5	22.6	28.9	25.5	34.5	43.1	46.3	35.8	13.1	6.5	6.9	4.5	277	8.46
G2	60199	4.4	15.8	24.8	24.7	37.7	43.5	41.7	30.3	9.7	1.6	1.2	1.4	237	14.26
G3	150138	0.9	8.6	19.5	23.4	31.4	36.9	30.2	14.3	2.6	0.4	0.1	0.1	168	25.27
G4	145588	3.3	8.9	14.7	12.1	17.4	21.0	20.8	15.6	4.8	2.4	1.6	3.0	126	18.29
H1	50910	3.3	7.2	28.6	46.8	47.8	38.1	23.4	4.1	2.7	2.9	7.0	4.3	216	11.01
H2	79967	1.4	7.1	25.4	39.2	34.6	29.4	14.2	1.4	0.9	0.9	2.8	1.4	159	12.68
I1	47493	3.5	18.1	19.4	19.3	21.5	26.5	28.5	20.6	4.9	1.7	1.4	0.8	166	7.90
I2	49784	1.3	10.0	18.3	17.5	16.1	19.4	20.5	9.4	1.7	0.7	0.6	0.3	116	5.76
J1	232969	1.4	4.8	17.7	25.3	24.7	25.4	21.3	8.2	2.0	0.9	1.6	0.9	134	31.26
J2	142815	1.8	2.7	12.1	16.8	19.8	17.8	8.9	2.7	5.0	4.8	4.8	1.2	99	14.08
Total annual precipitation water over the country															406

5. Conclusions

While with a long-term mean annual precipitation of 250 mm Iran is known as a semi-arid to arid country, she enjoys a very diverse climate. In this paper, we investigated the climate variability by mapping the precipitation diversity over the country, at three macro, meso, and micro-scales. Thirty-three years of the daily precipitation at 461 measuring stations are analyzed using CA (both hierarchical and non-hierarchical clustering) and PCA methods. The results demonstrate that at the macro-scale the regime of Iran's precipitation is mapped into six regions. The moist air masses entering the country are the main controlling factor. At a mesoscale, the precipitation regime is further mapped into ten zones. The occasional collision of the air masses creates the extra four zones. The six regions and the ten zones show the differently distinguished magnitude and annual patterns of precipitation. The six and ten zones are comparable to previous studies. At the micro-scale, 24 precipitation micro-zones are distinguished and introduced in this research for the first time. The vast area, complex topography and latitude variations of the country, and extensive nearby water bodies control such a precipitation diversity. While the pattern of the mean annual hyetograph of some micro-zones is the same, however, their monthly precipitation magnitude varies. The southeastern provinces of Sistan-Baluchestan with a long-term mean annual precipitation of 99 mm and the southwestern coast of the Caspian Sea with 1293 mm, are the driest and wettest zone in the country, respectively. The long-term monthly and annual magnitude and the annual distribution of precipitation at each micro-zone provide an accurate reference for water resources management in the country.

Declarations

Acknowledgment

Financial support provided by Shiraz University, Iran (grant no. 91GCU4M1206) is acknowledged. Precipitation data was collected from the archives of Fars Province Meteorological Organization (FPMO) and Fars Regional Water Authority (FRWA), Iran.

Declaration of Interest

The authors declare that they have no known competing financial interests or personal relationships that could have appeared to influence the work reported in this paper.

Authors distributions

Nozar Samani: Supervision,Conceptualization, Methodology, Project administration, funding acquisition, Writing-Reviewing and Editing; **Zahra Jamshidi:** Data curation, Software, Formal analysis, Writing- Original draft.

Funding Statement: as stated in the Acknowledgement section this research was funded by Shiraz University, Iran (grant no. 91GCU4M1206).

Availability of data: Precipitation data analyzed in this research are available from the corresponding author on reasonable request.

Ethics approval: The Authors declare that the research reported here has not been submitted/published elsewhere.

Consent to participate: Co-author (Miss Zahra Jamshidi) agrees and allows me to submit this article to *Theoretical and Applied Climatology*.

Consent to publish: Authors allow *Theoretical and Applied Climatology* to publish this article upon acceptance.

References

1. Alijani, B., 2000. Iran Climatology, 5th ed., Payam Nour Publication. Tehran, Iran, ISBN 978-964-455-621-0.
2. Alijani, B., O'Brien, J., Yarnal, B., 2008. Spatial analysis of precipitation intensity and concentration in Iran. Theoretical and Applied Climatology. 94(1), 107-124. https://doi.org/10.1007/s00704-007-0344-y
3. Alizadeh, F., Roushangar, K., Adamowski, J., 2019. Investigating monthly precipitation variability using a multiscale approach based on ensemble empirical mode decomposition. Paddy and Water Environment. 17(4), 741-759. https://doi.org/10.1007/s10333-019-00754-x
4. Baeriswyl, P. A., Rebetez, M., 1997. Regionalization of precipitation in Switzerland by means of principal component analysis. Theoretical and Applied Climatology. 58(1-2), 31-41. https://doi.org/10.1007/BF00867430
5. Balling, R. C., Keikhosravi Kiany, M. S., Sen Roy, S., Khoshhal, J., 2016. Trends in extreme precipitation indices in Iran: 1951–2007. Advances in Meteorology. 2016. https://doi.org/10.1155/2016/2456809
6. Bartlett, M. S., 1950. Tests of significance in factor analysis. British Journal of statistical psychology. 3(2), 77-85. https://doi.org/10.1111/j.2044-8317.1950.tb00285.x
7. Candeias, C., Da Silva, E. F., Salgueiro, A. R., Pereira, H. G., Reis, A. P., Patinha, C., Matos, J.X., Avila, P.H., 2011. The use of multivariate statistical analysis of geochemical data for assessing the spatial distribution of soil contamination by potentially toxic elements in the Aljustrel mining area (Iberian Pyrite Belt, Portugal). Environmental Earth Sciences. 62(7), 1461-1479.https://doi.org/10.1007/s12665-010-0631-2
8. Charrad, M., Ghazzali, N., Boiteau, V., Niknafs, A., 2012. NbClust Package: finding the relevant number of clusters in a dataset. J. Stat. Softw.
9. Darand, M., Daneshvar, M. R. M., 2014. Regionalization of precipitation regimes in Iran using principal component analysis and hierarchical clustering analysis. Environmental Processes. 1(4), 517-532. https://doi.org/10.1007/s40710-014-0039-1
10. Dinpashoh, Y., Fakheri-Fard, A., Moghaddam, M., Jahanbakhsh, S., Mirnia, M., 2004. Selection of variables for the purpose of regionalization of Iran's precipitation climate using multivariate methods. Journal of hydrology. 297(1-4), 109-123. https://doi.org/10.1016/j.jhydrol.2004.04.009
11. Domroes, M., Kaviani, M., Schaefer, D., 1998. An analysis of regional and intra-annual precipitation variability over Iran using multivariate statistical methods. Theoretical and Applied Climatology. 61(3-4), 151-159.https://doi.org/10.1007/s007040050060
12. Everitt, B.S., Landau, S., Leese, M., 2001. Cluster analysis, 4th edn. Arnold, London.
13. Ehrendorfer, M., 1987. A regionalization of Austria's precipitation climate using principal component analysis. Journal of Climatology. 7(1), 71-89. https://doi.org/10.1002/joc.3370070107
14. Fovell, R. G., Fovell, M. Y. C., 1993. Climate zones of the conterminous United States defined using cluster analysis. Journal of Climate. 6(11), 2103-2135. https://doi.org/10.1175/1520-0442(1993)006%3C2103:CZOTCU%3E2.0.CO;2
15. Gocic, M., Trajkovic, S., 2014. Spatio-temporal patterns of precipitation in Serbia. Theoretical and applied climatology. 117(3-4), 419-431. https://doi.org/10.1007/s00704-013-1017-7
16. Heydarizad, M., Raeisi, E., Sori, R., Gimeno, L., 2019. An overview of the atmospheric moisture transport effect on stable isotopes ($\delta\ ^{18}O$, $\delta\ ^{2}H$) and D excess contents of precipitation in Iran. Theoretical and Applied Climatology. 138(1), 47-63. https://doi.org/10.1007/s00704-019-02798-9
17. Hong, Y., Gochis, D., Cheng, J. T., Hsu, K. L., Sorooshian, S., 2007. Evaluation of PERSIANN-CCS rainfall measurement using the NAME event rain gauge network. Journal of Hydrometeorology. 8(3), 469-482. https://doi.org/10.1175/JHM574.1

18. Kassambara, A., 2017. Practical guide to cluster analysis in R: Unsupervised machine learning, 1st ed., STHDA (http://sthda.com).
19. Kaiser, H. F., 1970. A second-generation little jiffy. Psychometrika. 35(4), 401-415. https://doi.org/10.1007/BF02291817
20. Kidd, C., Huffman, G., 2011. Global precipitation measurement. Meteorological Applications. 18(3), 334-353. https://doi.org/10.1002/met.284
21. Knerr, I., Trachte, K., Garel, E., Huneau, F., Santoni, S., Bendix, J., 2020. Partitioning of Large-Scale and Local-Scale Precipitation Events by Means of Spatio-Temporal Precipitation Regimes on Corsica. Atmosphere. 11(4), 417. https://doi.org/10.3390/atmos11040417
22. Kottek, M., Grieser, J., Beck, C., Rudolf, B., Rubel, F., 2006. World map of the Köppen-Geiger climate classification updated. Meteorologische Zeitschrift, 15(3), 259-263.https://doi.org/10.1127/0941-2948/2006/0130
23. Lawson, R. G., Jurs, P. C., 1990. New index for clustering tendency and its application to chemical problems. Journal of chemical information and computer sciences. 30(1), 36-41. https://doi.org/10.1021/ci00065a010
24. MacQueen, J., 1967. Some methods for classification and analysis of multivariate observations. In Proceedings of the fifth Berkeley symposium on mathematical statistics and probability. 1(14), 281-297.
25. Madani, K., 2014. Water management in Iran: what is causing the looming crisis? Journal of environmental studies and sciences. 4(4), 315-328.https://doi.org/10.1007/s13412-014-0182-z
26. Mills, G. F., 1995. Principal component analysis of precipitation and rainfall regionalization in Spain. Theoretical and Applied Climatology. 50(3-4), 169-183. https://doi.org/10.1007/BF00866115
27. Modarres, R., 2006. Regional precipitation climates of Iran. Journal of Hydrology (New Zealand). 13-27.https://www.jstor.org/stable/43944936
28. Modarres, R., Sarhadi, A., 2011. Statistically-based regionalization of rainfall climates of Iran. Global and Planetary Change, 75(1-2), 67-75. https://doi.org/10.1016/j.gloplacha.2010.10.009
29. Nazemosadat, M. J., Samani, N., Barry, D. A., Molaii Niko, M., 2006. ENSO forcing on climate change in Iran: precipitation analysis. Iranian Journal of Science and Technology, Transaction B: Engineering, 30(ARTICLE), 555-565.
30. Rencher, A. C., Schimek, M. G., 1997. Methods of multivariate analysis. Computational Statistics. 12(4), 422-422.
31. Raziei, T., 2018. A precipitation regionalization and regime for Iran based on multivariate analysis. Theoretical and applied climatology. 131(3-4), 1429-1448. https://doi.org/10.1007/s00704-017-2065-1
32. Ribes, A., Thao, S., Cattiaux, J., 2020. Describing the relationship between a weather event and climate change: a new statistical approach. Journal of Climate. 33(15), 6297-6314.https://doi.org/10.1175/JCLI-D-19-0217.1
33. Richman, M. B., 1986. Rotation of principal components. Journal of climatology. 6(3), 293-335.https://doi.org/10.1002/joc.3370060305
34. Sabziparvar, A. A., Movahedi, S., Asakereh, H., Maryanaji, Z., Masoodian, S. A., 2015. Geographical factors affecting variability of precipitation regime in Iran. Theoretical and Applied Climatology. 120(1), 367-376. https://doi.org/10.1007/s00704-014-1174-3
35. Samani, N., Karimi, S., 2009. The spatial and temporal pattern of precipitation in Iran and its relation with ENSO. International Conference on Water Resources, F. Doulati (Ed.), 16-18 August 2009, Shahrood, Iran.https://civilica.com/doc/83108/
36. Sarmadi, F., Shokoohi, A., 2015. Regionalizing precipitation in Iran using GPCC gridded data via multivariate analysis and L-moment methods. Theoretical and applied climatology. 122(1-2), 121-128.https://doi.org/10.1007/s00704-014-1292-y
37. Soltani, S., Modarres, R., Eslamian, S. S., 2007. The use of time series modeling for the determination of rainfall climates of Iran. International Journal of Climatology. 27(6), 819-829.https://doi.org/10.1002/joc.1427
38. Srivastava, A., Grotjahn, R., Ullrich, P. A., Risser, M., 2019. A unified approach to evaluating precipitation frequency estimates with uncertainty quantification: Application to Florida and California watersheds. Journal of Hydrology. 578, 124095. https://doi.org/10.1016/j.jhydrol.2019.124095
39. Uddin, M. N., Islam, A. S., Bala, S. K., Islam, G. T., Adhikary, S., Saha, D., Haque, S., Fahad, M.G.R., Akter, R., 2019. Mapping of climate vulnerability of the coastal region of Bangladesh using principal component analysis. Applied geography. 102, 47-57.https://doi.org/10.1016/j.apgeog.2018.12.011
40. Vaghefi, S. A., Keykhai, M., Jahanbakhshi, F., Sheikholeslami, J., Ahmadi, A., Yang, H., Abbaspour, K. C., 2019. The future of extreme climate in Iran. Scientific reports. 9(1), 1-11. https://doi.org/10.1038/s41598-018-38071-8
41. White, D., Richman, M., Yarnal, B., 1991. Climate regionalization and rotation of principal components. International Journal of Climatology. 11(1), 1-25. https://doi.org/10.1002/joc.3370110102

Figures

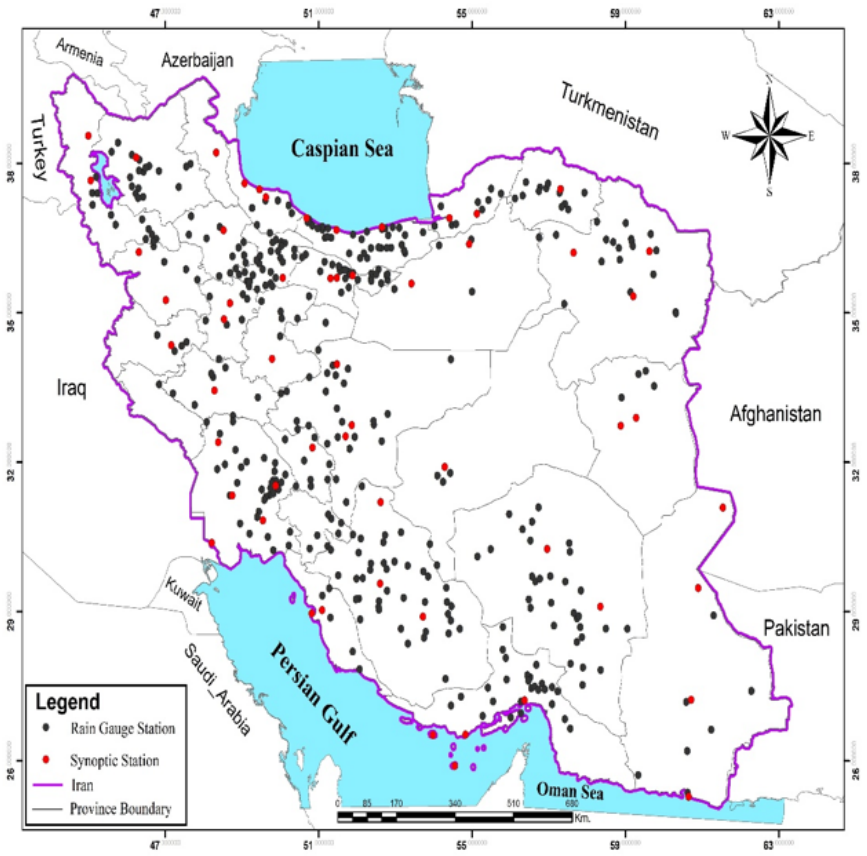

Figure 1

Location of the selected rain gauges and synoptic stations in Iran.

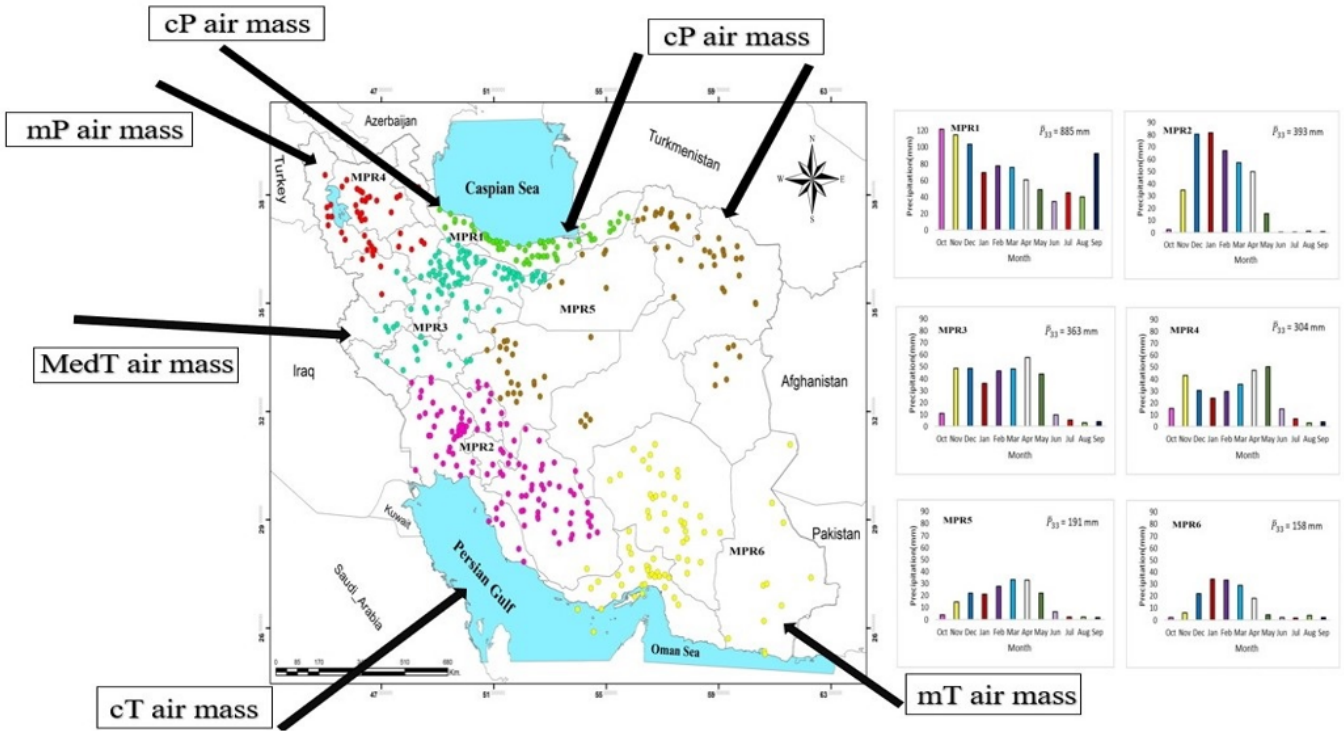

Figure 2

Macro-precipitation regions of Iran and the long-term mean annual hyetograph for 1983-2016 of each region. Major air masses entering the country: Continental Polar (cP) air mass from the north, Maritime Polar (mP) air mass from the northwest, Mediterranean (MedT) air mass from the West, Continental Tropical (cT) air mass from the south and southwest, Maritime Polar (mT) air mass from the southeast.

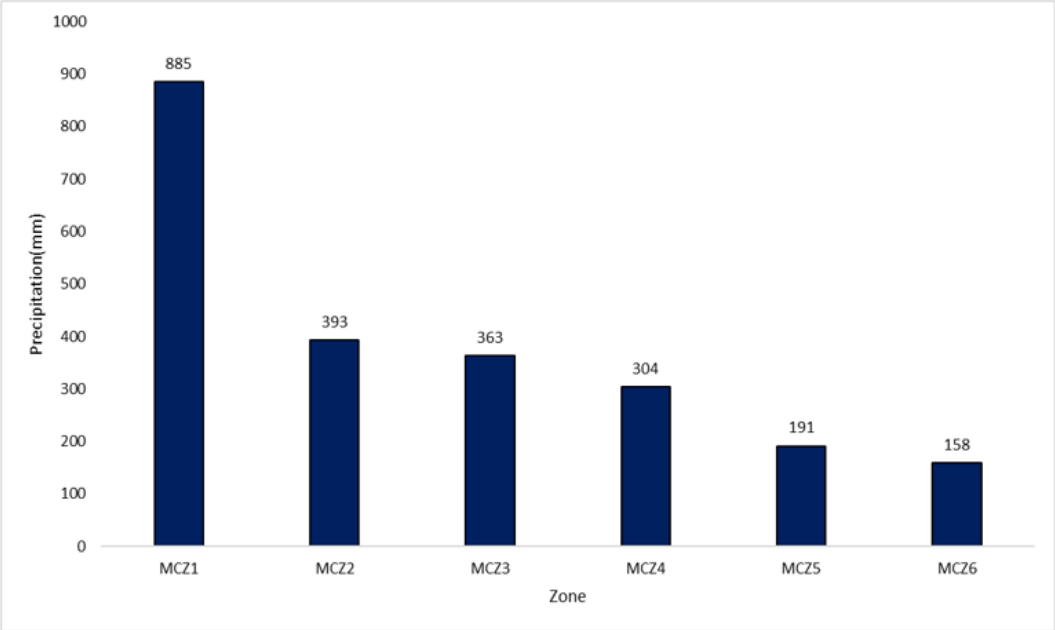

Figure 3

The long-term mean annual precipitation in the six macro-precipitation zones of Iran.

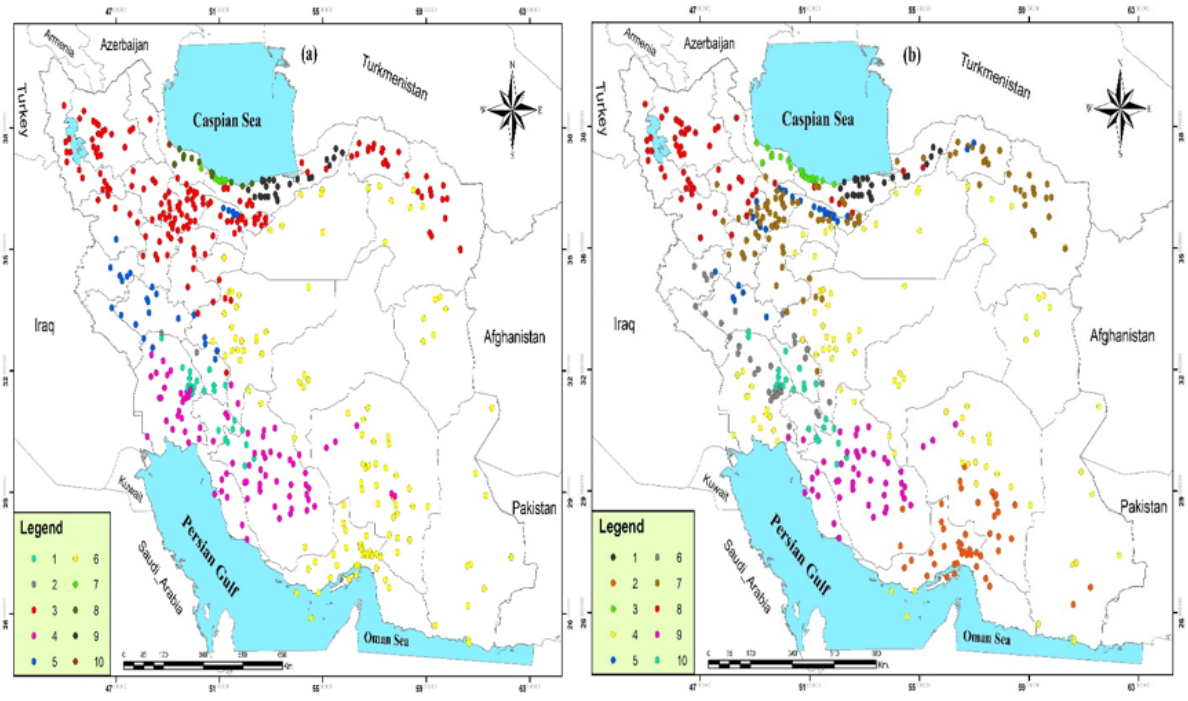

Figure 4

Meso-precipitation zones of Iran based on CA: a) Ward's method-Euclidean distance, b) K-Means Clustering.

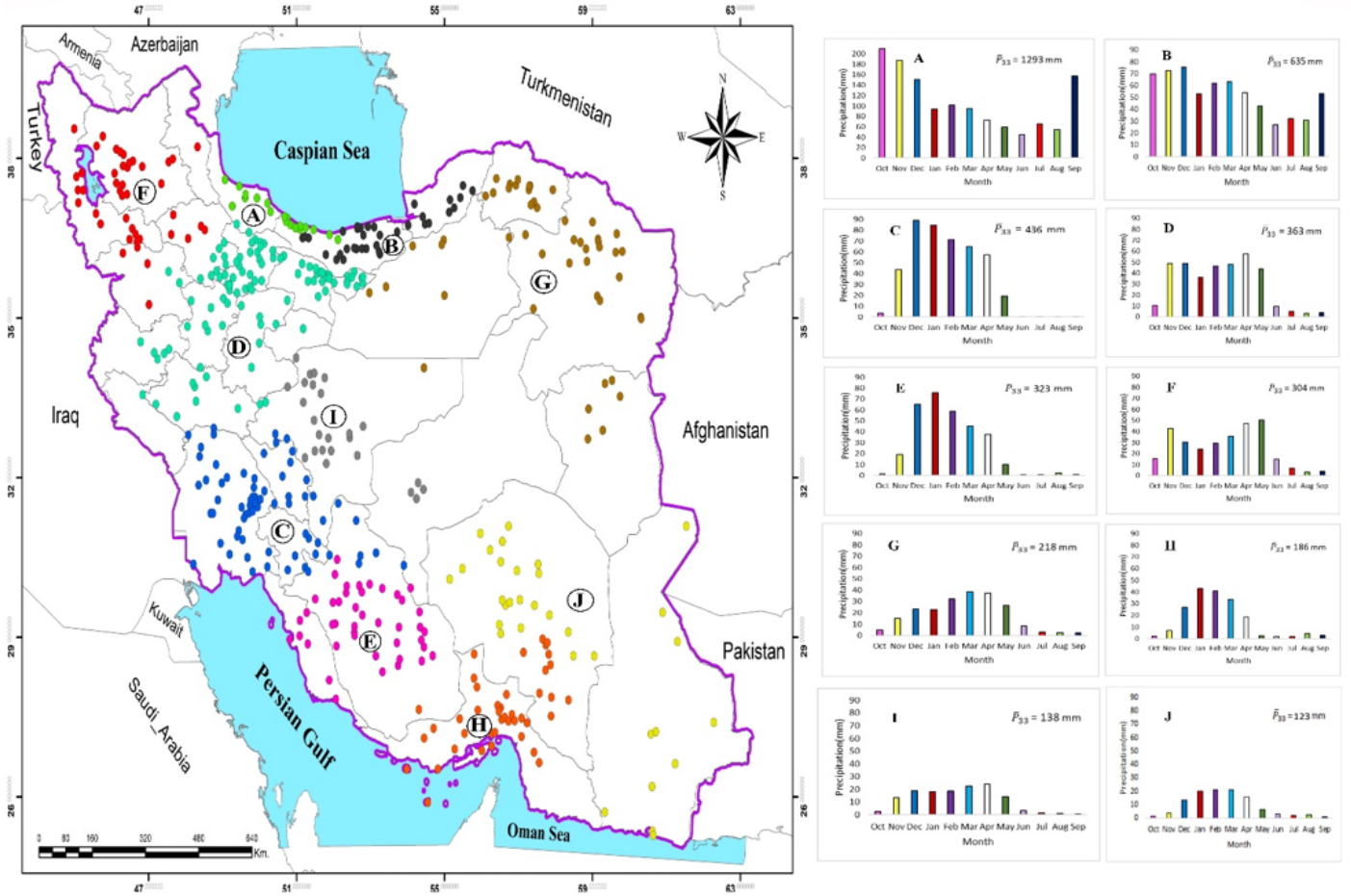

Figure 5

Meso-precipitation zones of Iran based on HCA (Ward's method-Pearson correlation) and the long-term mean annual hyetograph (1983-2016) of each zone. Note the variability of precipitation magnitude and distribution in each zone.

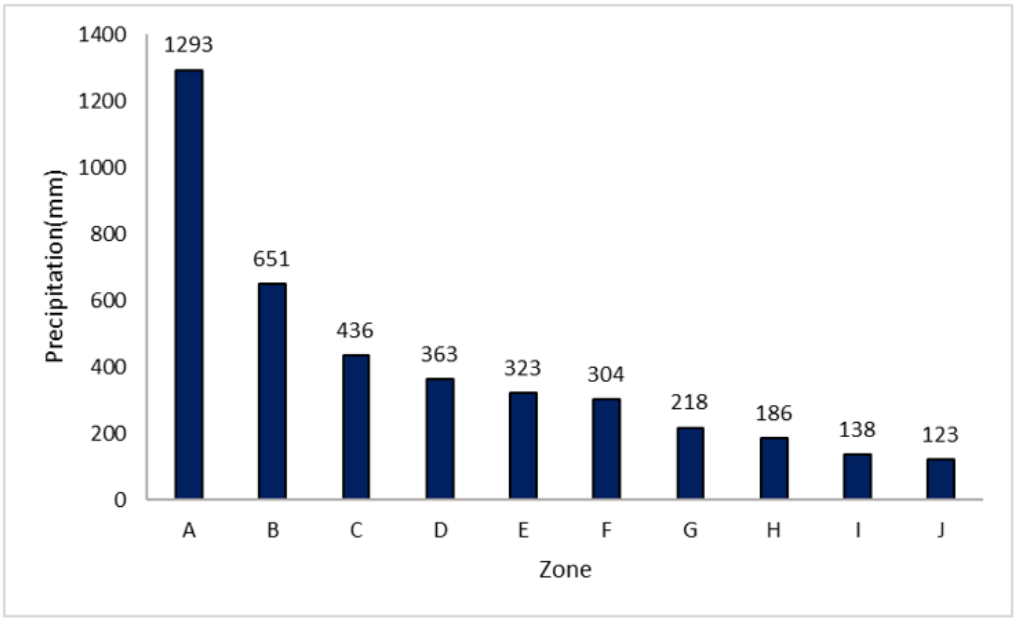

Figure 6

The long-term mean annual precipitation in ten meso-precipitation zones of Iran. The mean annual precipitation decreased from zone A to J.

Figure 7

The micro-precipitation zones of Iran obtained from a) K-Means Clustering, b) HCA (Ward's method-Euclidean Distance), c) HCA (Ward's method-Pearson correlation), and d) PCA.

Figure 8

The long-term mean annual hyetographs of the 24 micro-zones, (P_{33})¯ is the 33-year mean annual rainfall in each zone.

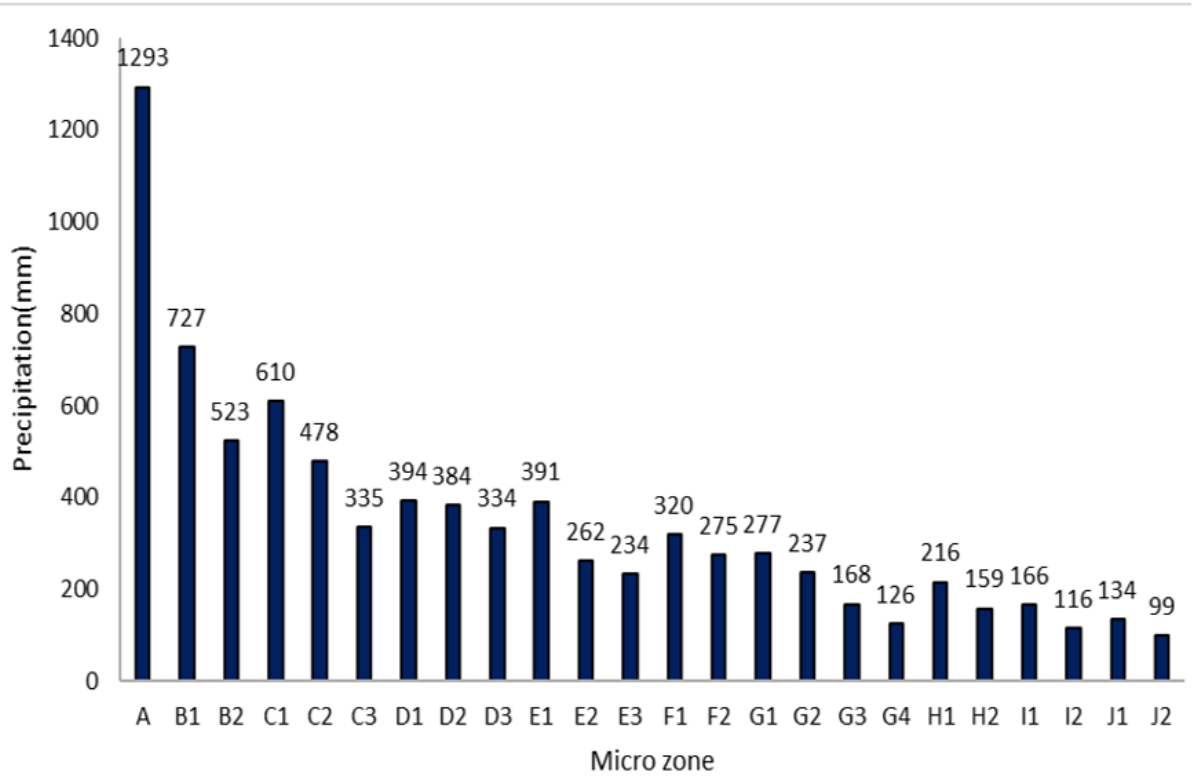

Figure 9

The long-term mean annual precipitation in the 24 micro-precipitation zones of Iran.

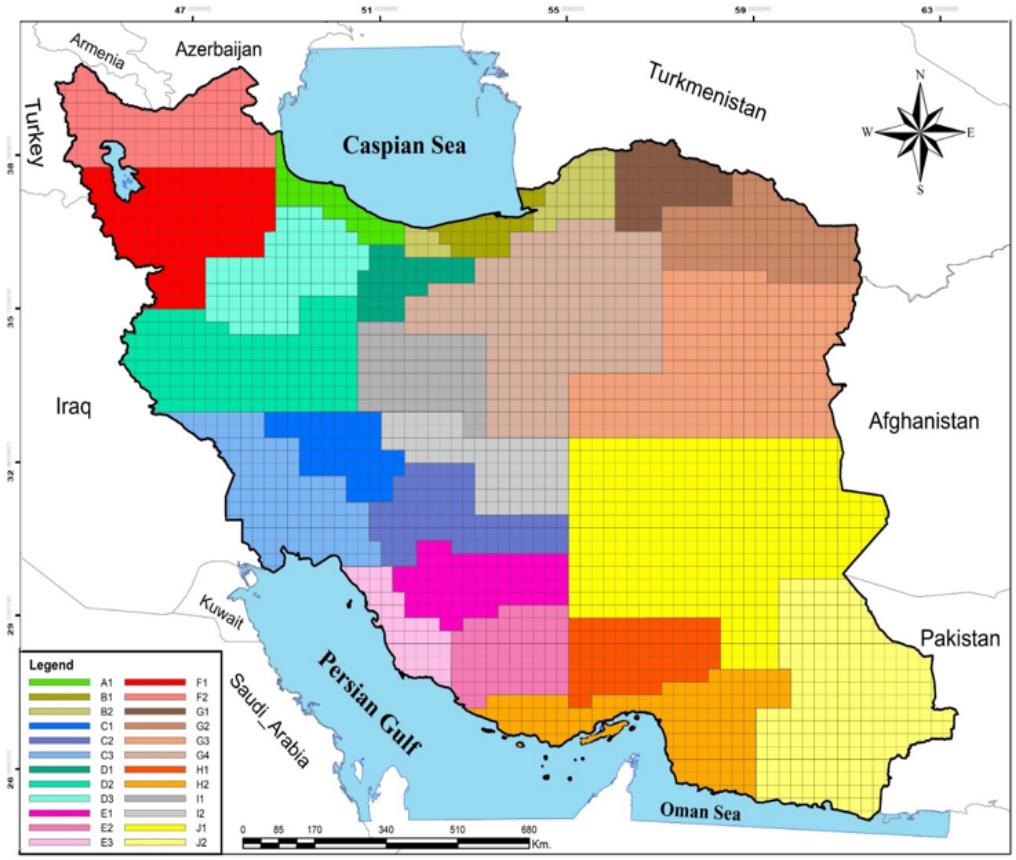

Figure 10

The micro-precipitation zones of Iran overlaid on a 0.25□gridded map.

Supplementary Files

This is a list of supplementary files associated with this preprint. Click to download.

- SupplementaryMaterials.docx